

# The *Drosophila* Fragile X Mental Retardation Protein Controls Actin Dynamics by Directly Regulating Profilin in the Brain

Simon P. Reeve,<sup>1</sup> Laura Bassetto,<sup>1</sup>  
Ginka K. Genova,<sup>2</sup> Yelena Klejner,<sup>2,3</sup>  
Maarten Leysen,<sup>1</sup> F. Rob Jackson,<sup>2,3</sup>  
and Bassem A. Hassan<sup>1,\*</sup>

<sup>1</sup>Laboratory of Neurogenetics  
Department of Human Genetics  
Flanders Interuniversity Institute for Biotechnology  
University of Leuven School of Medicine  
3000 Leuven  
Belgium

<sup>2</sup>Department of Neuroscience and  
Center for Neuroscience Research  
Tufts University School of Medicine  
Boston, Massachusetts 02111

<sup>3</sup>Sackler School Graduate Program in Genetics  
Tufts University School of Medicine  
Boston, Massachusetts 02111

## Summary

Loss of Fragile X mental retardation protein (FMRP) function causes the highly prevalent Fragile X syndrome [1, 2]. Identifying targets for the RNA binding FMRP is a major challenge and an important goal of research into the pathology of the disease. Perturbations in neuronal development and circadian behavior are seen in *Drosophila dfmr1* mutants. Here we show that regulation of the actin cytoskeleton is under dFMRP control. dFMRP binds the mRNA of the *Drosophila profilin* homolog and negatively regulates Profilin protein expression. An increase in Profilin mimics the phenotype of *dfmr1* mutants. Conversely, decreasing Profilin levels suppresses *dfmr1* phenotypes. These data place a new emphasis on actin misregulation as a major problem in *fmr1* mutant neurons.

## Results and Discussion

FMRP is a highly conserved RNA binding protein [3, 4]. The identification of a *Drosophila* homolog, dFMRP, opened the door to detailed genetic investigation of the physiological role of this protein. Altered morphology at the *Drosophila* neuromuscular junction was shown to be due to misregulation of Futsch, the fly homolog of the microtubule binding protein MAP1B [5]. However, *futsch* misregulation does not account for brain phenotypes in *dfmr1* mutants [6], suggesting that other targets are involved. Recently, *Drosophila* dRac1 has been shown to positively regulate dFMRP. On the other hand, Lee et al. [7], found that dFMRP may negatively regulate *dRac1* mRNA. These data suggest that Rac1 acts via dFMRP to control actin cytoskeletal dynamics. Crucially, however, the precise cellular role of dFMRP is unknown.

To identify FMRP targets in the brain, we initiated a Western immunoblot search for neuronal proteins regu-

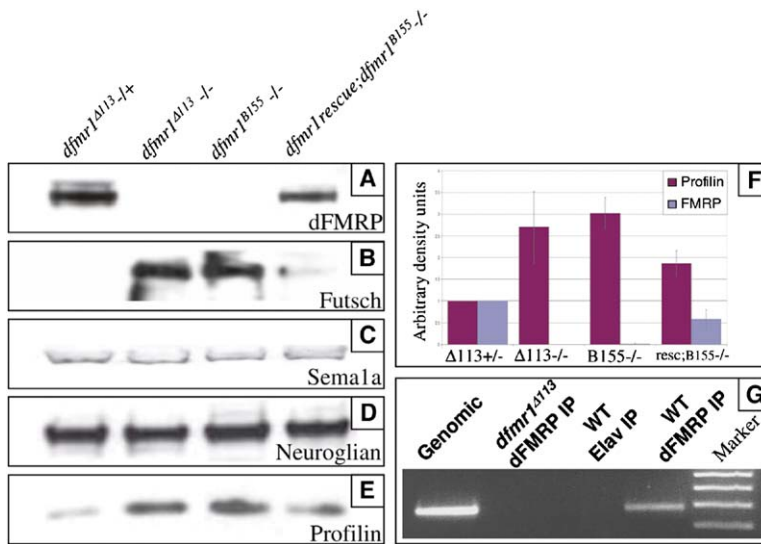
lated by dFMRP. We obtained 32 antibodies to neuronally expressed proteins with functions potentially relevant to *dfmr1* phenotypes. We tested for misregulation of these proteins in pharate adult brain extracts from two independently derived *dfmr1* mutants (*dfmr1*<sup>Δ113</sup> [5] and *dfmr1*<sup>B155</sup> [8]). We used Futsch upregulation as a positive control (Figure 1B). Of 16 antibodies with a signal in brain extracts, 12, including Semaphorin1a and Neuroglian, for example, showed normal abundance in *dfmr1* mutants (Figures 1C and 1D). Three other antibodies gave unclear results. However, we found *Drosophila* Profilin (encoded by *chickadee*) to be reproducibly strongly upregulated in the *dfmr1* mutants (Figures 1E and 1F). These results indicate that dFMRP negatively regulates Profilin. A genomic rescue construct (*P[w+=dfmr1]* [8]), which partially restores dFMRP in a mutant background (Figure 1A, lane 4), also partially rescues the misregulation of Profilin (Figures 1E and 1F). Notably, the ratio of Profilin in mutant versus rescued flies is comparable to the ratio of dFMRP itself in the two genotypes (Figure 1F; 1.67 versus 1.73), suggesting a sensitive response of Profilin to dFMRP levels.

Next, we investigated a physical interaction between dFMRP and *chickadee* mRNA in immunoprecipitates of dFMRP-RNP (ribonucleoprotein) complexes. Upon RT-PCR of the precipitated material, a band of the expected size is observed (Figure 1G, lane 4), indicating that *chickadee* mRNA is associated with dFMRP in vivo. We performed two controls to determine specificity: (1) We did not observe a PCR product with immunoprecipitates from *dfmr1* mutants (Figure 1G, lane 2); and (2) precipitates of the pan-neuronal RNA binding protein ELAV [9] also gave negative results (Figure 1G, lane 3).

To establish that these interactions are physiologically relevant, we investigated genetic interactions between *chickadee* and *dfmr1*. We first carefully documented neuronal-extension and branching defects of LNV neurons in *dfmr1* mutants [6, 10]. Specifically, we quantified defects in the morphology of collateral branches from the small LNV cells and assessed the posterior optic tract (POT), arising from the large LNV cells [11].

dFMRP has been proposed to function in a dose-dependent manner [10], an observation seen in mice [12], and recently reported for human patients [13]. In addition, the sensitive response of Profilin levels to dFMRP levels suggests a dose-dependent role for dFMRP in regulating actin dynamics. To determine if the ectopic collateral branches observed on the small LNV projections is dependent on dFMRP levels, we began by examining projections in the partial loss-of-function *dfmr1* mutant *EP*<sup>3517</sup> (with approximately 10% of wild-type levels [10]) and saw no collateral branches in heterozygotes, whereas 6% of homozygotes displayed one ectopic branch (Table 1). Similarly, an ectopic branch was observed in 15% and 12.5%, respectively, of homozygous mutants (Figures 2B and 2C; Table 1 and Figure 3). These defects were rescued by

\*Correspondence: bassem.hassan@med.kuleuven.ac.be



dFMRP from *dfmr1<sup>Δ113</sup>/TM6B* (lane 1, A) to that from *P[*dfmr1*];dfmr1<sup>B155</sup>* (lane 4, A) is 1.73. The ratio of Profilin levels in these genotypes is 1.67.

(G) *chickadee* mRNA coimmunoprecipitates with dFMRP. Lane 1: Expected size of *chickadee* PCR product from wild-type genomic DNA. Lane 2: Immunoprecipitation performed on homozygous *dfmr1<sup>Δ113</sup>* brains with dFMRP-specific antibody followed by RT-PCR on precipitated material. No *chickadee* mRNA is detected. Lane 3: Immunoprecipitation on wild-type brains with ELAV-specific antibody. No *chickadee* mRNA is detected. Lane 4: Immunoprecipitation performed on wild-type brains with dFMRP-specific antibody and subsequent RT-PCR with *chickadee*-specific primers. A product of the expected size is clearly detectable.

a *dfmr1<sup>+</sup>* genomic transgene (Figure 2D; Table 1 and Figure 3), indicating that ectopic branching is dependent on dFMRP levels and providing a sensitive assay for genetic interactions.

While studying the dorsal projections of the small LNV, we noted that the tightly fasciculated commissure of the large LNV neurons, or posterior optic tract (POT), displayed a defasciculation (split) phenotype. We quantified this to determine if it correlates with dFMRP levels. A split phenotype is defined as defasciculation along more than 25% of POT length (Figure 2E). We observed a dose-dependent increase in the incidence of POT splitting, with a 3-fold higher split phenotype seen in null homozygotes compared to hypomorphic *EP<sup>3517</sup>* homozygotes (Figures 2F and 2G; Table 1 and Figure 3). This phenotype was rescued in flies with a genomic *dfmr1* transgene (Figure 2H; Table 1 and Figure 3). Therefore, the dose of dFMRP is important for the integrity of the LNV POT.

Next we tested if POT splitting and ectopic branching defects are modulated by increasing Profilin dosage. We used two previously described duplication chromosomes (henceforth Dp) overlapping the *chickadee* gene [14, 15], as well as expression of a Profilin cDNA via the UAS/Gal4 system. The rationale is that if dFMRP represses Profilin, then increasing Profilin levels in a *dfmr1*-deficient background ought to enhance the *dfmr1* phenotypes. Conversely, increasing dFMRP should suppress Profilin gain of function.

*dfmr1* and Profilin Dp heterozygotes show no ectopic branching (Figures 2A and 2I; Table 1 and Figure 3). In contrast, 28% of *Dp/+;dfmr1/+* double heterozygotes showed a collateral branch (Figures 2K and 2M; Table 1 and Figure 3). This phenotype was rescued by a *dfmr1<sup>+</sup>* transgene (Figure 2L; Table 1 and Figure 3).

Figure 1. dFMRP Binds to and Regulates the Translation of Profilin mRNA

Fly heads from *dfmr1<sup>Δ113</sup>/TM6B* (lane 1), *dfmr1<sup>Δ113</sup>/dfmr1<sup>Δ113</sup>* (Lane 2), *dfmr1<sup>B155</sup>/dfmr1<sup>B155</sup>* (lane 3), and *P[w<sup>+</sup>=dfmr1];dfmr1<sup>B155</sup>* (lane 4) were subjected to PAGE and immunoblotted (n = 3).

(A) No dFMRP was seen in either the *dfmr1<sup>Δ113</sup>* homozygotes or the *dfmr1<sup>B155</sup>* homozygotes. The rescued *dfmr1<sup>B155</sup>* (lane 4) show a lower amount of dFMRP than the *dfmr1<sup>Δ113</sup>* heterozygotes (lane 1). (B) Futsch protein is upregulated with loss of dFMRP.

(C and D) No difference was observed with either (C) *Sema1a* or (D) *Neuroglian* protein levels across the different genotypes.

(E) Profilin protein levels increase with dFMRP loss. This can be specifically rescued with the addition of two genomic *dfmr1*-rescue fragments (compare lanes 3 and 4).

(F) Graph showing densitometry of dFMRP (blue) and Profilin (red) (n = 3). The ratio of

A second assay for genetic interaction between *chickadee* and *dfmr1* is POT fasciculation. Flies carrying the Dp alone showed a weak split phenotype (Table 1), suggesting that this phenotype is sensitive to Profilin levels. Strikingly, 90% of *Dp/+;dfmr1/+* flies showed a split phenotype (Figures 2K and 2M; Table 1 and Figure 3). Furthermore, the POT split in *Dp/+;dfmr1/+* flies generally extended the entire length of the commissure, whereas it extended to no further than 50% of the commissure in *dfmr1* mutants (Table 1). This phenotype was rescued with the *dfmr1<sup>+</sup>* transgene (Figure 2L; Table 1 and Figure 3).

To test the cell autonomy of *chickadee-dfmr1* interactions and exclude a role for other genes within the duplication chromosomes, we expressed Profilin cDNA [16] in the LNV neurons. We observed a split phenotype in 47.6% of the brains examined (n = 21). Importantly, this phenotype was rescued when we coexpressed Profilin and dFMRP (n = 9, p = 0.006).

Schenck et al. [17] proposed that dRac1, a known regulator of actin dynamics [18, 19], positively regulates dFMRP. We assayed for genetic interactions between *dfmr1* and *dRac1* in the LNV. We found that heterozygotes for *dRac1* [18] displayed 17% penetrance of the collateral branch and a 33% penetrance of the split phenotype (Table 1). Heterozygous *dfmr1* flies displayed no collateral branches and an 8% penetrance of the POT split (Table 1). However, *dfmr1/dRac1* exhibited complete penetrance of both phenotypes (Figure 2N; Table 1). If *dRac1* interacts positively with *dfmr1*, it should interact negatively with Profilin. Indeed, all *Dp/+;dRac1/+* flies show both phenotypes (Figure 2O; Table 1). These data support the hypothesis that dRac1 and dFMRP act cooperatively to negatively regulate Profilin.

Loss of *dfmr1* causes extensive coverage of the

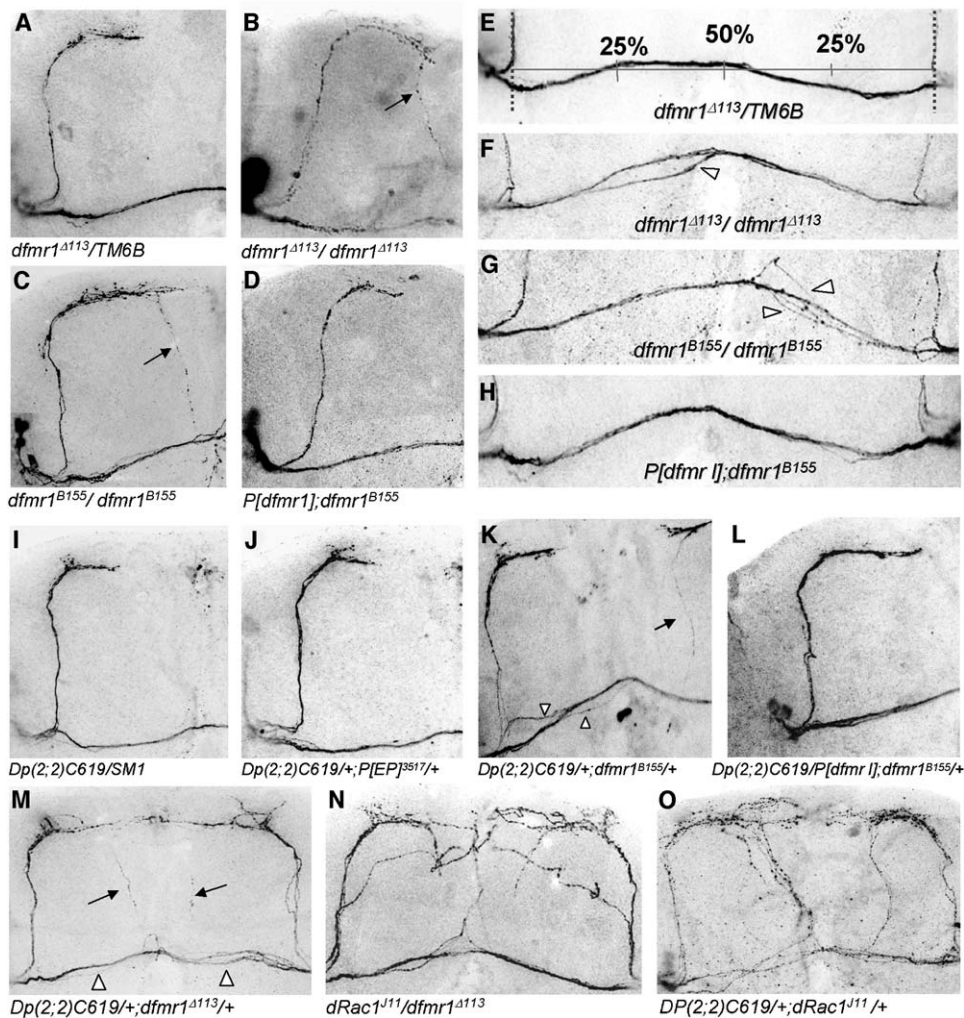


**Figure 2. *dfmr1* Mutants Show Dose-Sensitive Collateral Branching and Defasciculation of the Posterior Optic Tract (POT) of LNV's**

(A–D) Half brains from adult flies of stated genotypes were stained with anti-PAP antibody. Ectopic collateral branches are indicated with arrows. (A) A *dfmr1<sup>Δ113</sup>/TM6B* adult brain showing no collateral branching. (B) A *dfmr1<sup>Δ113</sup>/dfmr1<sup>Δ113</sup>* adult brain displaying collateral branching with an axon turning ventrally and extending toward the POT ( $p < 0.05$  to controls). (C) A *dfmr1<sup>B155</sup>/dfmr1<sup>B155</sup>* adult brain displaying collateral branching similar to that seen in (B) ( $p < 0.05$  to controls). (D) A rescued *P[dfmr1];dfmr1<sup>B155</sup>* adult half brain showing no collateral branching.

(E–H) POT-splitting phenotypes are indicated by arrowheads. Length of POT was defined as percentage of length along the intersection of a vertical line drawn from the dorsal projections (dotted line) with a horizontal line, as exemplified in (E). (E) Almost all *dfmr1<sup>Δ113</sup>/TM6B* brains display normal POT morphology. (F) A *dfmr1<sup>Δ113</sup>/dfmr1<sup>Δ113</sup>* adult brain showing POT splitting ( $p < 0.05$  to controls). (G) A *dfmr1<sup>B155</sup>/dfmr1<sup>B155</sup>* adult brain showing a POT-splitting phenotype ( $p < 0.05$  to controls). (H) A *P[dfmr1];dfmr1<sup>B155</sup>*-rescue fly brain showing no POT-splitting phenotype ( $p = 0.01$  to null).

(I) Half brain from *Dp(2;2)C619/SM1* showing no collateral branching or POT splitting.

(J) Half brain from *Dp(2;2)C619/+;P[EP]<sup>3517</sup>/+* displaying no collateral branching or POT splitting.

(K) Half brain from *Dp(2;2)C619/+;dfmr1<sup>B155</sup>/+* displaying collateral branching (arrows) and POT splitting (arrowheads) ( $p < 0.005$  to controls).

(L) Half brain from a rescued *Dp(2;2)C619/P[dfmr1];dfmr1<sup>B155</sup>/+* fly showing no collateral branching or POT splitting ( $p < 0.002$  to [K] and [M]).

(M) *Dp(2;2)C619/+;dfmr1<sup>Δ113</sup>/+* brain showing collateral branching and POT splitting ( $p < 0.005$  to controls).

(N) Brain from *dRac1<sup>J11</sup>/dfmr1<sup>Δ113</sup>* displaying multiple and severe disruptions to LNV morphology. (O) Brain from *Dp(2;2)C619/+;dRac1<sup>J11</sup>/+* showing severe morphological disruptions to the LNVs.

target area by LNV dorsal-projection termini (Figures 4A and 4B [6]). This increase could result from (1) an increase in the number of dorsal branches, (2) an increase in branch order, (3) an increased extension of the dorsal branches, or (4) any combination thereof. We counted the branch number and found no increase in mutants ( $6.3 \pm 0.4$ ) as compared to wild-type flies

( $7.3 \pm 0.3$ ). In addition, we saw little or no secondary branching in either genotype (data not shown). To determine if the increase in area coverage was due to increased branch extension, we first quantified target area coverage in wild-type flies, genetic-background controls, and mutant flies (see Experimental Procedures; Figure 4H). We found genetic-background

Table 1. Penetrance of Collateral-Branching and POT-Splitting Phenotypes and Severity of POT Splitting in Various Genotypes

Genotype	Collateral Branching (Percent of Total Half Brains)	POT Splitting (Percent of Total Brains Showing >25% Split)
P[EP] <sup>3517</sup> /TM6B (n = 9)	0%	0%
dfmr1 <sup>Δ113</sup> /TM6B (n = 12)	0%	8% (1/12)
P[EP] <sup>3517</sup> /P[EP] <sup>3517</sup> (n = 9)	6% (1/18)	22% (2/9)
dfmr1 <sup>Δ113</sup> /dfmr1 <sup>Δ113</sup> (n = 13)	15% (4/26)	69% (9/13)
dfmr1 <sup>B155</sup> /dfmr1 <sup>B155</sup> (n = 12)	12.5% (3/24)	58% (7/12)
P[dfmr I]/P[dfmr I];dfmr1 <sup>B155</sup> /dfmr1 <sup>B155</sup> (n = 11)	4.5% (1/22)	36% (4/11)
Dp(2;2)C619/SM1 (n = 13)	0%	31% (4/13)
Dp(2;2)C619/+; P[EP] <sup>3517</sup> /+ (n=7)	0%	29% (2/7)
Dp(2;2)C619/+;dfmr1 <sup>Δ113</sup> /+ (n = 11)	27% (6/22)	91% (10/11)
Dp(2;2)C619/+;dfmr1 <sup>B155</sup> /+ (n = 7)	29% (4/14)	85% (6/7)
Dp(2;2)C619/P[dfmr I]; dfmr1 <sup>B155</sup> /+ (n = 9)	0%	0%
Dp(2;2)C619/+;dRac1 <sup>J11</sup> /+ (n = 14)	100% (28/28)	100% (14/14)
dRac1 <sup>J11</sup> /dfmr1 <sup>Δ113</sup> (n = 14)	100% (28/28)	93% (13/14)
dRac1 <sup>J11</sup> /+ (n = 6)	17% (2/12)	33% (2/6)

*n* values are given in parentheses with each genotype. The number of samples displaying the phenotype is given in parenthesis with the percentage. See also the chart in Figure 3.

controls to be indistinguishable from wild-type flies. Both mutant and *Dp/+;dfmr1/+* brains showed greater area coverage than wild-type flies or controls because of a combination of increased dorso-ventral and medio-lateral extension (Figures 4H, 4I, and 4J). If dFMRP negatively regulates Profilin, then the phenotype of *dfmr1* mutants ought to be rescued by decreasing Profilin. Indeed, heterozygosity for *chic* significantly reduced area coverage in *dfmr1* mutants (Figure 4C).

To test cell autonomy, we expressed dFMRP and Profilin specifically in LNV neurons by using *UAS-dfmr1*<sup>+</sup>, *UAS-chic*, and *Pdf-Gal4* [20] and quantified LNV dorsal branching by using a specific antibody [21]. Flies overexpressing dFMRP almost completely lack normal target innervation, whereas those overexpressing Profilin cover a target area significantly larger than that of controls (Figures 4E, 4E', and 4H). If dFMRP downregu-

lates Profilin, then increasing Profilin should rescue the phenotype of *dfmr1* overexpression. Indeed, flies expressing dFMR1 and Profilin showed area coverage similar to that of controls (Figures 4G and 4H). Taken together, our data suggest that dFMRP and Profilin interact physically and genetically to ensure normal neurite fasciculation and extension and, therefore, correct target innervation.

To determine if the relationship between dFMRP and Profilin is relevant for neuronal populations other than the LNVs, we analyzed the mushroom bodies (MBs). Michel et al. [22] and Pan et al. [23] showed that *dfmr1* controls growth of MB axonal processes. Consistently, we observed that FMRP overexpression in MBs significantly increases the gap between the β lobes. We also found a striking increase in the gap between the γ lobes (Figures 4K, 4L, and 4N). If dFMRP causes these phe-

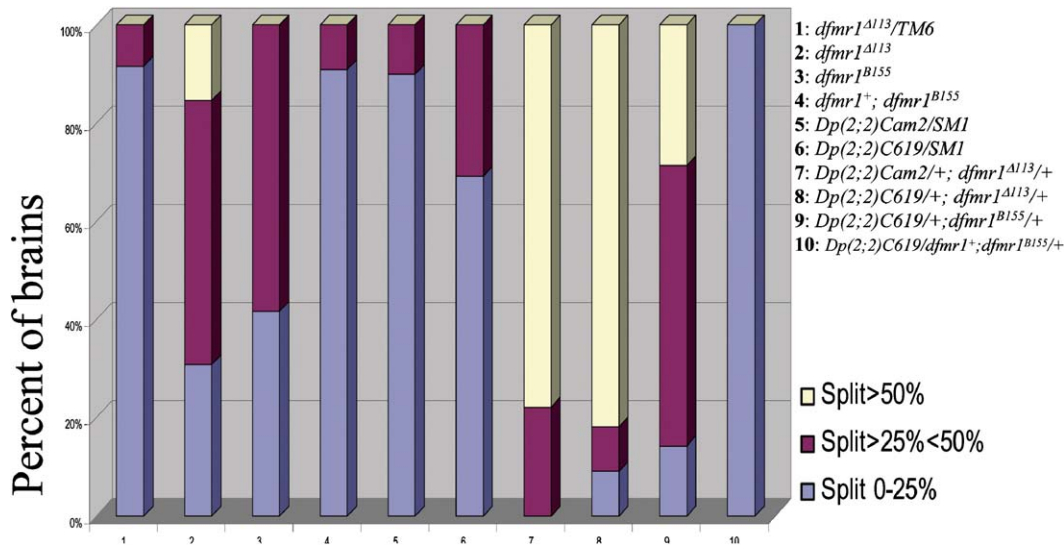
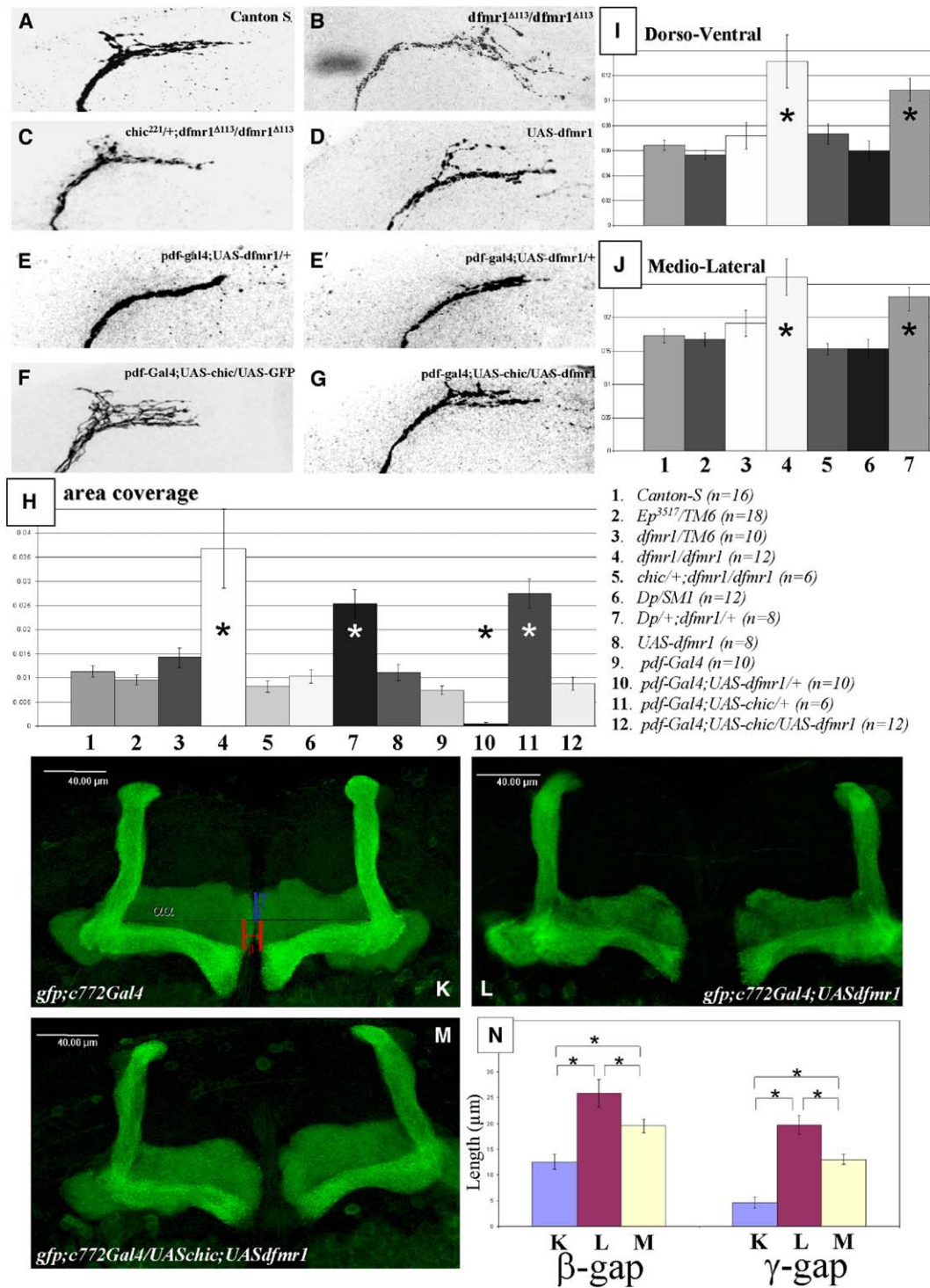


Figure 3. Chart of Data in Table 1

The severity of the POT-splitting phenotype is shown in the graph as follows: Blue = between 0% and 25% split; purple = between 25% and 50% split; yellow = greater than 50% split.



**Figure 4. dFMRP and *chickadee* Interact Cell Autonomously to Regulate Dorsal-Projection-Area Coverage and Mushroom-Body Development** (A–J) Tips of the LNV dorsal projections from adult half brains stained with either anti-PAP (A–E and G) or anti-GFP (F). (A)–(G) show representative samples of the given genotypes. (C) shows that rescue of the mutant increased area coverage ( $n = 6$ ,  $p = 4.6 \times 10^{-5}$ ). (E) shows the predominant phenotype of *pdf-Gal4;UAS-dfmr1*, and (E') shows the maximal branching observed. (H) The target-area coverage (see [Experimental Procedures](#)) for each genotype was compared to Canton S wild-type controls (mean area of 0.011 au, standard deviation [SD] = 0.005). Significant changes (\*) were observed in *dfmr1/dfmr1* (mean = 0.036, SD = 0.029,  $p < 0.05$ ), *Dp/+;dfmr1/+* (mean = 0.025, SD = 0.008,  $p < 0.01$ ), *pdf-Gal4;UAS-dfmr1* (mean = 0.008, SD = 0.0045,  $p = 4.6 \times 10^{-5}$ ), and *pdf-Gal4;UAS-chic/+* (mean = 0.027, SD = 0.007,  $p = 0.002$ ). No other genotypes significantly differed. (I) An increase in target-area width (see [Experimental Procedures](#)) compared to that of controls (mean = 0.064, SD = 0.016) was observed for *dfmr1/dfmr1* (mean = 0.13, SD = 0.07,  $p = 0.05$ ) and *Dp/+;dfmr1/+* (mean = 0.11, SD = 0.025,  $p < 0.01$ ). (J) An increase in target-area length (see [Experimental Procedures](#)) as compared to that of controls (mean = 0.17, SD = 0.043) was seen for *dfmr1/dfmr1* (mean = 0.26, SD = 0.09,  $p < 0.05$ ) and *Dp/+;dfmr1/+* (mean = 0.23, SD = 0.044,  $p = 0.02$ ).

notypes by suppressing Profilin, then coexpressing Profilin and dFMRP should reduce the severity of these phenotypes. Combining Profilin and dFMRP significantly rescued dFMRP overexpression phenotypes (Figures 4L, 4M, and 4N). Therefore, the dFMRP-Profilin interaction is not restricted to the LNV.

Flies homozygous for *dfmr1* null alleles have arrhythmic locomotor activity [6, 10]. Based on differences between neuroanatomical and behavioral defects in *dfmr1* mutants, we proposed that the two phenotypes are independently regulated by dFMRP [10]. The neuroanatomical defects in *Dp/+;dfmr1/+* flies provided the opportunity to test this hypothesis. Indeed, *Dp/+;dfmr1/+* flies manifested normal activity rhythms (Figure S1 and Table S1), suggesting that dFMRP may independently regulate neuronal morphology and function, although it is possible that our neuroanatomical assays are more sensitive than the behavioral assays.

The aim of this work was to identify dFMRP targets in brain neurons. Our molecular and genetic studies demonstrate that dFMRP binds the *profilin* (*chickadee*) mRNA, suggesting direct regulation of Profilin. Although Profilin appears not to have been identified in large-scale searches for mammalian FMRP targets [24], it would be interesting to examine if it is misregulated in FMRP mutant mouse brains. Using LNV and MB neurons, we show that (1) upregulation of Profilin is sufficient to mimic phenotypes caused by loss of *dfmr1*, (2) that overexpression of dFMRP in the LNV is rescued by upregulation of Profilin, and (3) that reducing Profilin levels rescues phenotypes observed in *dfmr1* mutants.

Profilin regulates filamentous actin dynamics by facilitating filament turnover and providing a pool of ATP-actin for filament polymerization [25]. Our results indicate that the interaction between Profilin and dFMRP contributes to the correct patterning of *Drosophila* brain neurons; i.e., dFMRP has a direct role in regulating the neuronal actin cytoskeleton. Schenck et al. [17] showed that dRac1 inhibits CYFIP, an inhibitor of dFMRP. This implies a positive relationship, with dRac1 activating dFMRP to inhibit Profilin translation. However, Lee et al. [7] suggest that dFMRP acts as a negative regulator of *dRac1* mRNA, and thus it is possible to envisage a feedback mechanism whereby dFMRP represses excessive Profilin translation (Figure S2A). With loss of dFMRP, the fine control of Profilin and actin dynamics becomes disrupted (Figure S2B). Signaling via dRac1 activates dFMRP to regulate Profilin and other cytoskeletal proteins. To maintain sensitivity to these signals, dFMRP suppresses its own activation by repression of *dRac1* translation. The inhibition of dFMRP consequently releases the repression of *dRac1* translation and thereby restores the system's sensitivity (Figure S2C). Our data suggest a need for a paradigm shift toward

misregulation of the actin network as an important factor in Fragile X syndrome.

## Experimental Procedures

### Fly Strains and Genetics

Canton S was used as the wild-type control. The *dfmr1*<sup>Δ113</sup> allele, the *P[EP]<sup>3517</sup>* parental line, and the *UAS-dfmr1* lines were obtained from A. Bailey and G. Rubin at the University of California and are described in [5]. The *dfmr1*<sup>B155</sup> allele and *p[dfmr1\*];dfmr1*<sup>B155</sup> lines were obtained from H. Siomi and are described in [8]. *Dp(2;2)C619* (region 26A1–7;28E) is a tandem duplication spanning the *chickadee* locus (26A09–26B01) [12, 14, 15] and was obtained from the Bloomington stock center. *Dp(2,2)Cam2* (region 23D01–02;26C01–02) overlaps *Dp(2;2)C619* at 26A;26C01–02 [15] and was obtained from the Bloomington Stock center. *UAS-chic* overexpression lines were a kind gift from L. Cooley. The *c772-Gal4* driver was obtained from R. Davis. The *Pdf-Gal4* driver was obtained from P. Taghert and is described in [20]. All crosses were performed on standard fly food at controlled ambient temperature (22°C–23°C) except the overexpression crosses, which were performed at 25°C.

### SDS-PAGE Analysis

For protein analysis, total protein was extracted from whole fly heads by homogenization in loading buffer (SDS, bromophenol blue, glycerol, and β-mercaptoethanol) and heating to 98°C for 5 min. The crude extract was separated by SDS-PAGE in a 4%–12% NuPAGE novex bis-tris gel (Invitrogen) and electroblotted onto Hybond-ECL membrane (Amersham). All monoclonal antibodies were obtained from the Developmental Studies Hybridoma Bank (DSHB; University of Iowa, department of biological sciences, Iowa City, IA 52242). dFMRP was probed with monoclonal 5A11; Neuroglian was probed with monoclonal BP104; and Profilin was probed with monoclonal chi1J. Sema1a antibody was a kind gift from A. Kolodkin. Primary antibodies were detected by the appropriate horseradish-peroxidase-coupled secondary antibodies (Amersham) by the chemiluminescent method (ECL kit, Amersham).

### Immunoprecipitations and RT-PCR

Approximately 100 pharate adult heads from wild-type (CS) or homozygous *dfmr1*<sup>Δ113</sup> flies were dissected in extraction buffer consisting of 50 mM Tris (pH 8.0), 0.5% Triton X-100, 1 mM DTT, 100 units/ml RNase out, 0.2% vanadyl ribonucleoside complex, 1 mM PSMF, and 10 μl/ml protease inhibitor cocktail (Sigma, catalog number 8340).

All further manipulations were carried out at 4°C. The tissues were homogenized in the same buffer, and the precleared cell lysates were used for immunoprecipitation.

Protein A-Sepharose beads (Sigma) were mixed for 2 hr with 10 μl of anti-dFMRP (5A11 antibody from the DSHB) or with 10 μl of anti-Elav-antibody (9F8A9 antibody from the DSHB). The antibody-bead mix was then washed with buffer NT2 (50 mM Tris [pH 7.4]; 150 mM NaCl; 1 mM MgCl<sub>2</sub>; 0.05% Nonidet P-40). Immunoprecipitation was carried out for 2 hr in 1 ml volume with buffer NT2R (NT2 containing the following additions: 100 units/ml RNase out, 0.2% vanadylribonucleoside complex, 20 mM EDTA, and 1 mM DTT). The immunoprecipitate was washed four times with NT2R, twice with NT2 containing 1 M urea, and twice with high-stringency NT2 buffer (50 mM Tris [pH 7.4], 50 mM NaCl, 1 mM MgCl<sub>2</sub>, and 0.05% Nonidet P-40). The antibody-bead-protein mixture was phenol/chloroform extracted once, and RNA in the samples was ethanol precipitated (glycogen was used as a carrier). To amplify

(K–N) dFMRP and *chickadee* interaction is required for normal mushroom-body development. (K) Confocal stack of a *gfp;c772-Gal4* mushroom body. Measurements of the β lobe gap (average of 12.5 μm; red lines) and γ lobe gap (average of 4.6 μm; blue lines) were taken (n = 12). Values were normalized against α lobe to α lobe (black arrow). (L) An increase in β lobe gap and γ lobe gap is seen in *gfp;c772-Gal4;UAS-dfmr1* mushroom bodies (average of 25.9 μm for β gap and 19.7 μm for γ gap; n = 11, p = 2.3 × 10<sup>−5</sup> [β], 3.8 × 10<sup>−5</sup> [γ]). (M) *gfp;c772-Gal4/UAS-chic;UAS-dfmr1* show a significant rescue compared to (L) (average β gap of 19.5 μm [p = 0.01] and γ gap of 12.9 μm [p < 0.001], n = 8). The scale bar represents 40 μm. (N) Graph of mean gap distance between the β lobes and the mean gap distance between the γ lobes: blue = *c772-Gal4*; purple = *c772/+;UAS-dfmr1/+*; yellow = *c772/UAS-chic;UAS-dfmr1/+*. Error bars indicate standard error of the mean (SEM). An asterisk indicates p < 0.05.

RNAs precipitated with dFMRP-RNPs, we used the RiboAmp HS RNA amplification kit (Arcturus) according to the manufacturer's directions. Although we could not detect cDNA by spectrophotometry after one round of amplification, we proceeded with a polymerase chain reaction (PCR) amplification. PCR primers were designed to amplify a 287 bp segment near the 3' end of the *chickadee* gene. The primers were as follows: 5'-GTT TCG ATC TAC GAG GAT CCC-3' (forward) and 5'-CCG CAA ATT CTT TCT TGG CCG-3' (reverse). We used the entire sample from a single dFMRP-RNP or Elav-RNP immunoprecipitation (8  $\mu$ l volume). For genomic DNA PCR reactions, we used 95 ng of CS genomic DNA.

#### Immunohistochemistry

Immunohistochemistry was performed as previously described [10]. Antibodies used were as follows: anti-PAP at 1/1000 (donated by P. Taghert); anti-GFP at 1/1000 (Molecular Probes); Fluorescence-conjugated secondary antibodies at 1/500 (Molecular Probes).

#### Analyses of LNV Neurons

After labeling with anti-PAP, LNVs were scored in a blind fashion as follows. (1) Collateral branches: Scores were given for half brains with PDF-labeled axons that could be traced to the dorsal projections but did not follow the normal dorsal-projection trajectory. (2) POT splits: A commissure was regarded as "split" if it displayed separation over more than a quarter of the length. (3) Coverage of the dorsal-projection area: Two measurements were made for all genotypes—the distance from the point of defasciculation to the most medial extent of each axon, averaged for all axons in one sample and referred to as the "target-area length," and the "target-area width," defined as the distance between the most dorsal arbor (excluding the dorsal horn) and the most ventral arbour, medial to the branch start point. Values were corrected against POT length (which shows no significant differences between genotypes [data not shown]). The "maximal area" coverage was calculated by multiplying uncorrected target-area length by uncorrected target-area width, then correcting for the square of the POT length. Samples were compared to *Canton S*.

#### Analysis of Mushroom Bodies

1- to 2-day-old adult brains were immunolabeled with anti-GFP (Molecular Probes) or anti-FasII (monoclonal 22C10, Developmental Studies Hybridoma Bank). Confocal Z sections were obtained for all brains with a Leica TCS SP2 system. All measurements were performed with Leica Confocal Software. The intersection formed by the medial edge of the  $\alpha$  lobes with the dorsal edge of the  $\beta$  lobes was defined for both sides of the mushroom bodies. The distance between these points was taken as "brain size" and was statistically similar for all genotypes. The lengths of the  $\gamma$  lobes, the  $\beta$  lobes, and the gap span of the respective lobes were taken relative to this line. Lengths of  $\gamma$  lobes and  $\beta$  lobes were statistically the same for all genotypes.

#### Statistical Analyses

Genotypes were compared by one- and two-tailed t tests with Statistica software (Statsoft [2001] STATISTICA [data-analysis software system] version 6.0). When multiple comparisons were performed, p values were corrected according to the Bonferroni step-down (Holm) method.

#### Behavioral Analysis

Locomotor activity data were acquired with Trikinetics monitors and the *Drosophila* Activity Monitoring (DAM) acquisition software (see [22]). Flies were entrained for 5–7 days in LD 12:12 at 24°C and then allowed to free run in constant darkness for 10–12 days. Activity records were analyzed with a MATLAB-based software package called Flytoolbox [16]. The robustness of rhythmicity was determined with the rhythmicity index (RI); flies with RI values >0.1 were considered rhythmic. The circadian period was calculated with the third peak of the autocorrelation function [16].

#### Supplemental Data

An additional two figures and one table are available with this article online at <http://www.current-biology.com/cgi/content/full/15/12/1156/DC1/>.

#### Acknowledgments

We thank the Bloomington Stock Center, the Developmental Studies Hybridoma Bank, and Drs. P. Taghert, H. Siomi, L. Cooley, G. Dreyfuss, J. Tyler, S. Hirose, A. Kolodkin, H. Lipshitz, T. Heino, and K. Miller for materials and S. Aerts for assistance with statistics. This work was supported by a Marie Curie Postdoctoral Fellowship (S.P.R.), a Fragile X Research Foundation grant and the Flanders Interuniversity Institute for Biotechnology (VIB) (B.A.H.), the National Institutes of Health (grant HL59873 to F.R.J.), the Center for Neuroscience Research at Tufts University School of Medicine/New England Medical Center, and the Tufts/Tufts-New England Medical Center Gastroenterology Research on Absorptive and Secretory Processes (GRASP) Center. We thank Natalie DeGeest and Mary Roberts for technical assistance, and Ira Espuny-Camacho for discussions.

Received: September 22, 2004

Revised: May 13, 2005

Accepted: May 13, 2005

Published: June 21, 2005

#### References

1. Chiurazzi, P., Neri, G., and Oostra, B.A. (2003). Understanding the biological underpinnings of fragile X syndrome. *Curr. Opin. Pediatr.* 15, 559–566.
2. Bakker, C.E., and Oostra, B.A. (2003). Understanding fragile X syndrome: Insights from animal models. *Cytogenet. Genome Res.* 100, 111–123.
3. Wan, L., Dockendorff, T.C., Jongens, T.A., and Dreyfuss, G. (2000). Characterisation of dFMR1, a *Drosophila melanogaster* homologue of the fragile X mental retardation protein. *Mol. Cell. Biol.* 20, 8536–8547.
4. Darnell, J.C., Jensen, K.B., Jin, P., Brown, V., Warren, S.T., and Darnell, R.B. (2001). Fragile X mental retardation protein targets G quartet mRNAs important for neuronal function. *Cell* 107, 489–499.
5. Zhang, Y.Q., Bailey, A.M., Matthies, H.J., Renden, R.B., Smith, M.A., Speese, S.D., Rubin, G.M., and Brodie, K. (2001). *Drosophila* fragile X-related gene regulates the MAP1B homolog Futsch to control synaptic structure and function. *Cell* 107, 591–603.
6. Dockendorff, T.C., Su, H.S., McBride, S.M., Yang, Z., Choi, C.H., Siwicki, K.K., Sehgal, A., and Jongens, T.A. (2002). *Drosophila* lacking *dfmr1* activity show defects in circadian output and fail to maintain courtship interest. *Neuron* 34, 973–984.
7. Lee, A., Li, W., Xu, K., Bogert, B.A., Su, K., and Gao, F.-B. (2003). Control of dendritic development by the *Drosophila* fragile X-related gene involves the small GTPase Rac1. *Development* 130, 5543–5552.
8. Inoue, S., Shimoda, M., Nishinokubi, I., Siomi, M.C., Okamura, M., Nakamura, A., Kobayashi, S., Ishida, N., and Siomi, H. (2002). A role for the *Drosophila* fragile X-related gene in circadian output. *Curr. Biol.* 12, 1331–1335.
9. Robinow, S., and White, K. (1991). Characterisation and spatial distribution of the ELAV protein during *Drosophila melanogaster* development. *J. Neurobiol.* 22, 443–461.
10. Morales, J., Hiesinger, P.R., Schroeder, A.J., Kume, K., Verstreken, P., Jackson, F.R., Nelson, D.L., and Hassan, B.A. (2002). *Drosophila* fragile X protein, DFXR, regulates neuronal morphology and function in the brain. *Neuron* 34, 961–972.
11. Helfrich-Förster, C. (1995). The period clock gene is expressed in central nervous system neurons which also produce a neuropeptide that reveals the projections of circadian pacemaker cells within the brain of *Drosophila melanogaster*. *Proc. Natl. Acad. Sci. USA* 92, 612–616.
12. Peier, A.M., McIlwain, K.L., Kenneson, A., Warren, S.T., Paylor,

- R., and Nelson, D.L. (2000). (Over)correction of FMR1 deficiency with YAC transgenics: Behavioural and physical features. *Hum. Mol. Genet.* 9, 1145–1159.
13. Menon, V., Leroux, J., White, C.D., and Reiss, A.L. (2004). Frontostriatal deficits in fragile X syndrome: Relation to FMR1 gene expression. *Proc. Natl. Acad. Sci. USA* 101, 3615–3620.
  14. Wills, Z., Marr, L., Zinn, K., Goodman, C.S., and Van Vactor, D. (1999). Profilin and the Abl tyrosine kinase are required for motor axon outgrowth in the *Drosophila* embryo. *Neuron* 22, 291–299.
  15. Boquet, I., Boujemaa, R., Carlier, M.-F., and Prèat, T. (2000). Ciboulot regulates actin assembly during *Drosophila* brain metamorphosis. *Cell* 102, 797–808.
  16. Verheyen, E.M., and Cooley, L. (1994). Profilin mutations disrupt multiple actin-dependent processes during *Drosophila* development. *Development* 120, 717–728.
  17. Schenck, A., Bardoni, B., Langmann, C., Harden, N., Mandel, J.-L., and Giangrande, A. (2003). CYFIP/Sra-1 controls neuronal connectivity in *Drosophila* and links the Rac1 GTPase pathway to the fragile X protein. *Neuron* 38, 887–898.
  18. Ng, J., Nardine, T., Harms, M., Tzu, J., Goldstein, A., Sun, Y., Dietzl, G., Dickson, B.J., and Luo, L. (2002). Rac GTPases control axon growth, guidance and branching. *Nature* 416, 442–447.
  19. Hakeda-Suzuki, S., Ng, J., Tzu, J., Dietzl, G., Sun, Y., Harms, M., Nardine, T., Luo, L., and Dickson, B.J. (2002). Rac function and regulation during *Drosophila* development. *Nature* 416, 438–442.
  20. Park, J.H., Helfrich-Förster, C., Lee, G., Liu, L., Rosbash, M., and Hall, J.C. (2000). Differential regulation of circadian pacemaker output by separate clock genes in *Drosophila*. *Proc. Natl. Acad. Sci. USA* 97, 3608–3613.
  21. Renn, S.C., Park, J.H., Rosbach, M., Hall, J.C., and Taghert, P.H. (1999). A pdf neuropeptide gene mutation and ablation of Pdf neurons each cause severe abnormalities of behavioural circadian rhythms in *Drosophila*. *Cell* 99, 791–802.
  22. Michel, C.I., Kraft, R., and Restifo, L.L. (2004). Defective neuronal development in the mushroom bodies of *Drosophila* Fragile X mental retardation 1 mutants. *J. Neurosci.* 24, 5789–5809.
  23. Pan, L., Zhang, Y.Q., Woodruff, E., and Broadie, K. (2004). The *Drosophila* Fragile X gene negatively regulates neuronal elaboration and synaptic differentiation. *Curr. Biol.* 14, 1863–1870.
  24. Brown, V., Jin, P., Ceman, S., Darnell, J.C., O'Donnell, W.T., Tenenbaum, S.A., Jin, X., Feng, Y., Wilkinson, K.D., Keene, J.D., et al. (2001). Microarray identification of FMRP-associated brain mRNAs and altered mRNA translational profiles in Fragile X syndrome. *Cell* 107, 477–487.
  25. dos Remedios, C.G., Chhabra, D., Kekic, M., Dedova, I.V., Tsubakihara, M., Berry, D.A., and Nosworthy, N.J. (2003). Actin binding proteins: Regulation of cytoskeletal microfilaments. *Physiol. Rev.* 83, 433–473.